Atherosclerosis Plus 55 (2024) 21–30

Contents lists available at ScienceDirect

Atherosclerosis Plus

journal homepage: www.elsevier.com/locate/atherosclerosis

Acute myocardial infarction preferentially alters low-abundant, long-chain unsaturated phospholipid and sphingolipid species in plasma high-density lipoprotein subpopulations

Maharajah Ponnaiah [a,1], Emile Zakiev [b,c,1], Marie Lhomme [a,1], Fabiana Rached [d], Laurent Camont [b], Carlos V. Serrano Jr. [d], Raul D. Santos [d,e], M. John Chapman [b], Alexander Orekhov [c,f,g], Anatol Kontush [b,*]

[a] IHU ICAN (ICAN OMICS and ICAN I/O), Foundation for Innovation in Cardiometabolism and Nutrition (ANR-10-IAHU-05), Paris, France
[b] National Institute for Health and Medical Research (INSERM), UMRS 1166 ICAN, Faculty of Medicine Pitié-Salpêtrière, Sorbonne University, Paris, France
[c] Institute of General Pathology and Pathophysiology, Moscow, Russia
[d] Heart Institute (InCor), University of Sao Paulo Medical School Hospital, Sao Paulo, Brazil
[e] Hospital Israelita Albert Einstein, Sao Paulo, Brazil
[f] Institute for Atherosclerosis Research, Moscow, Russia
[g] Centre of Collective Usage, Institute of Gene Biology, Moscow, Russia

ARTICLE INFO

Keywords:
HDL
Subpopulations
Lipidomics
Lipidome
Phospholipids
Sphingolipids
Acute myocardial infarction

ABSTRACT

Aim: High-density lipoprotein (HDL) particles in ST-segment elevation myocardial infarction (STEMI) are deficient in their anti-atherogenic function. Molecular determinants of such deficiency remain obscure.
Methods: Five major HDL subpopulations were isolated using density-gradient ultracentrifugation from STEMI patients (n = 12) and healthy age- and sex-matched controls (n = 12), and 160 species of phosphatidylcholine, lysophosphatidylcholine, phosphatidylethanolamine, phosphatidylinositol, phosphatidylglycerol, phosphatidylserine, phosphatidic acid, sphingomyelin and ceramide were quantified by LC-MS/MS.
Results: Multiple minor species of proinflammatory phosphatidic acid and lysophosphatidylcholine were enriched by 1.7–27.2-fold throughout the majority of HDL subpopulations in STEMI. In contrast, minor phosphatidylcholine, phosphatidylglycerol, phosphatidylinositol, phosphatidylethanolamine, sphingomyelin and ceramide species were typically depleted up to 3-fold in STEMI vs. control HDLs, while abundances of their major species did not differ between the groups. Intermediate-to-long-chain phosphatidylcholine, phosphatidylinositol and phosphatidylglycerol species were more affected by STEMI than their short-chain counterparts, resulting in positive correlations between their fold decrease and the carbon chain length. Additionally, fold decreases in the abundances of multiple lipid species were positively correlated with the double bond number in their carbon chains. Finally, abundances of several phospholipid and ceramide species were positively correlated with cholesterol efflux capacity and antioxidative activity of HDL subpopulations, both reduced in STEMI vs controls. KEGG pathway analysis tied these species to altered glycerophospholipid and linoleic acid metabolism.
Conclusions: Minor unsaturated intermediate-to-long-chain phospholipid and sphingolipid species in HDL subpopulations are most affected by STEMI, reflecting alterations in glycerophospholipid and linoleic acid metabolism with the accumulation of proinflammatory lysolipids and maintenance of homeostasis of major phospholipid species.

1. Introduction

Myocardial infarction (MI), one of the most frequent adverse events that can occur to an average individual in modern societies, usually results from plaque buildup in coronary arteries in a process of atherosclerosis [1]. Progression of atherosclerosis is accelerated by both high

* Corresponding author: INSERM Research Unit 1166 – ICAN, Faculty of Medicine Pitié-Salpêtrière, Sorbonne University, 91, bd de l'Hôpital, 75013 Paris, France.
E-mail address: anatol.kontush@sorbonne-universite.fr (A. Kontush).
[1] These authors equally contributed to the manuscript.

https://doi.org/10.1016/j.athplu.2023.12.001
Received 1 June 2023; Received in revised form 30 November 2023; Accepted 1 December 2023
Available online 15 December 2023

concentrations of low-density lipoprotein cholesterol (LDL-C) and low concentrations of high-density lipoprotein cholesterol (HDL-C) [2]. Moreover, low HDL-C concentrations are associated with increased risk of MI, though many patients with MI display normal HDL-C levels, indicating that HDL-C is a poor marker of defective HDL metabolism in inflammatory states involving MI [3]. This observation can be attributed, at least in part, to deficient antiatherogenic activities of HDL particles, which may include subnormal efflux of intracellular cholesterol from macrophages [4] together with compromised antioxidative [5], anti-apoptotic [6] and vasodilatory [7,8] actions. Indeed, reduced cholesterol efflux capacity of HDL is associated with incident cardiovascular disease in individuals on statin therapy [9]. In addition, increased oxidative potential of HDL is associated with premature MI [10]. The atheroprotective role of HDL may even evolve into pro-atherogenic under conditions of increased systemic inflammation as occurs in acute MI, hampering protective effects of HDL towards endothelium [11] as reflected by increased abundances of serum amyloid A and other inflammatory proteins in HDL from acute coronary syndrome (ACS) patients [12,13].

Anti-atherogenic HDL particles are however highly heterogeneous in their structure, composition and function [14], reflecting distinct metabolic pathways. Small, dense, protein-rich HDLs are distinguished by potent anti-atherogenic properties which are defective in ACS as documented in our previous study [15]. Such functional impairment is paralleled by alterations in the content of several classes of phosphosphingolipids across HDL particle subpopulations in patients with ST-segement elevation myocardial infarction (STEMI) relative to healthy controls. These alterations primarily include elevated content of lysophosphatidylcholine (LPC) and phosphatidic acid (PA) at the expense of other phospholipids. Consistent with these data, phosphatidylcholine (PC), sphingomyelin (SM) and plasmalogens are typically depleted in AMI HDL, while LPC is enriched [16–21]. These compositional alterations involve enrichment in saturated fatty acids (SFAs) at the expense of polyunsaturated fatty acids (PUFAs). Interestingly, similar abnormalities, including elevated content of LPC and SFA paralleled by reduced content of plasmalogens, SM, phospholipid and PUFAs, occur in HDL obtained from patients with Type 2 diabetes and Metabolic Syndrome which are major risk factors for AMI [22,23].

Of particular interest remain, however, possible roles for HDL function of individual (lyso)phosphosphingolipid species which could have evaded our attention in the class-wise analysis of the HDL lipidome in STEMI. When this question was addressed in our present study, we found that minor, unsaturated, intermediate-to-long-chain (lyso)phosphosphingolipid species of HDL subpopulations were primarily affected by STEMI, content of a few of them specifically correlating with defective antiatherogenic activities of HDL.

2. Materials and methods

Details of subjects, blood samples, isolation and characterisation of HDL subpopulations and lipidomics are available elsewhere [15] as well as in Online Supplement.

Data are shown as mean ± SD or median (25–75 percentiles) when appropriate. Between-group differences were analyzed using Mann-Wilcoxon *U* test. Pearson's product moment correlations were calculated to evaluate relationships between variables. For all statistical tests, $p < 0.05$ (Benjamini-Hochberg adjusted) was considered statistically significant.

Circular heatmaps were constructed by performing *t*-test between the STEMI and control groups. Only lipid species whose abundances significantly differed between the groups were colored. Bubble plots were employed to show quantitative information about mean abundances for all molecular species in HDL subpopulations from the STEMI group. Forest plots were built to convey information about the structure of fatty acid residues of affected lipid species, notably the length of carbon chains and the number of double bonds. Network maps were created in order to reveal relationships between the lipidome and function of HDL. Thickness of a connection between two nodes was proportional to the value of a correlation coefficient between them. The network maps were plotted using Cytoscape (version 3.7.0) with the plug-in MetScape (version 3.1.1).

Affected metabolic pathways were defined and included in the classical pathway representation after identification using the MetExplore web-based tool [24].

3. Results

3.1. HDL subpopulations were specifically enriched in PA and LPC species and depleted of PC, SM and Cer species in STEMI

STEMI patients featured atherogenic dyslipidemia involving significantly reduced plasma levels of HDL-C and apolipoprotein (apo) A-I and significantly elevated plasma levels of glucose and high-sensitivity C-reactive protein (hsCRP) relative to sex- and age-matched healthy normolipidemic controls as reported by us earlier [15]. The HDL lipidome was markedly perturbed in STEMI patients, with total PA and LPC increased and total Cer decreased in HDL subpopulations as earlier reported [15].

When abundances of lipid species were analyzed, all HDL subpopulations revealed significant differences between STEMI patients and healthy controls. However, the number of significantly differing between the groups species varied greatly across the HDL subpopulations for all lipid classes, including PC (from 7 to 9), SM (from 5 to 9), LPC (from 0 to 8), PI (from 0 to 5), PE (from 0 to 4), PS (from 0 to 2), Cer (from 1 to 11), PA (from 6 to 8) and PG (from 0 to 1) species (Tables S1 and S2 from Data Supplement). The small, dense HDL3b subfraction was most affected presenting 53 species with significantly altered abundance, followed by HDL2a, 3c, 2b and 3a, presenting 50, 42, 34 and 23 such species, respectively.

The circular heatmap illustrates arrangement of clusters produced by data analyses (Fig. 1A and B). When the heatmap was built for the differences in the abundances of lipid species between STEMI and control subjects, a distinct pattern was consistently observed across all HDL subpopulations. Notably, abundances of PA and LPC species were typically elevated in STEMI HDLs as compared to their counterparts from controls, while the content of PC, SM and Cer species was decreased. Profiles of other five phospholipid subclassess revealed mixed patterns, with species overrepresented and underrepresented in STEMI HDLs making up comparable shares. The most prominent and consistent differences were found throughout HDL subpopulations for PC 36:2, 36:5 and 40:8 and SM 32:2 and 41:2 (which were all significantly decreased by up to 0.37, 1.07, 1.66, 1.85 and 0.69-fold ($p < 0.001$) in STEMI vs control subjects; Fig. 1A and B and Tables S1 and S2 from Data Supplement) as well as for LPC 16:0, 20:3 and 20:4, and PA 34:1, 34:2, 36:4, and 38:4 (all increased by up to 1.70, 2.18, 2.16, 2.51, 3.00, 4.63 and 3.70-fold, respectively, $p < 0.001$, vs controls).

To assess whether these findings were specific to STEMI, we studied a group of patients with Metabolic Syndrome who similarly featured atherogenic dyslipidemia but did not reveal acute phase response. Again, all HDL subpopulations revealed significant differences between STEMI patients and healthy controls (Fig. 1, C). The number of significantly differing between the groups species varied greatly across lipid classes, from PS (up to 10) to Cer (up to 5) to SM and PG (up to 2) to PE and PI (up to 1). Strikingly, no difference in the abundances of PC, PA and LPC species was observed between the groups in any HDL subpopulation, providing a clear distinction from the alterations observed in STEMI HDLs. The small, dense HDL3c subfraction was most affected presenting 18 species with significantly altered abundance, followed by HDL3a, 3b, 2a and 2b, presenting 13, 9, 6 and 4 such species, respectively. Abundances of Cer, PG and PE species were typically elevated in STEMI HDLs as compared to their counterparts from controls, while the content of PS species was decreased. The most prominent and consistent

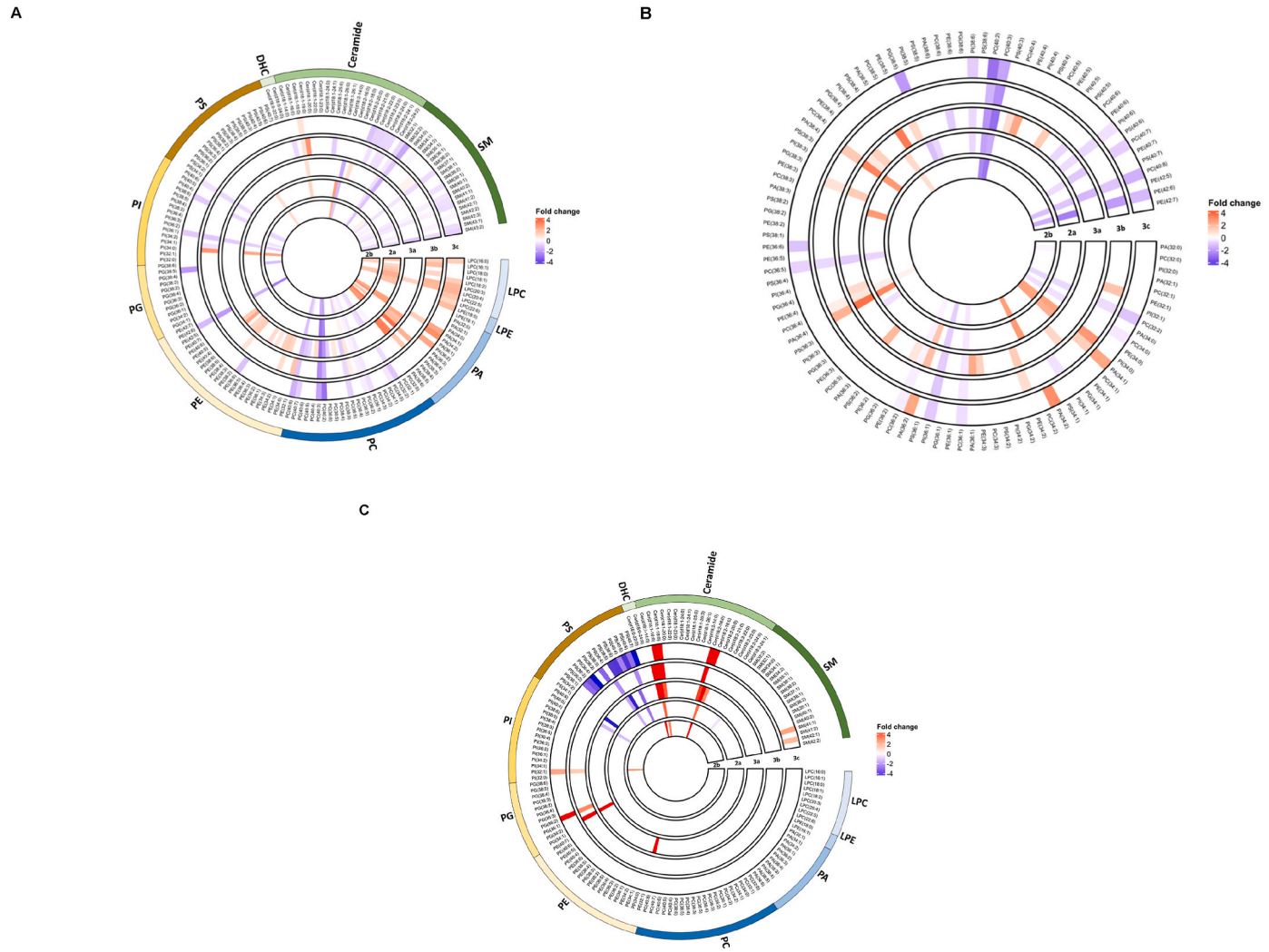

Fig. 1. Circular heatmap of the abundances of lipid species in the lipidome of HDL subpopulations of STEMI patients (A, B) and Metabolic Syndrome patients (C) relative to healthy controls. Data obtained in individual HDL subpopulations are shown as concentric circles of increasing size from large, light HDL2b to small, dense HDL3c. Abundance of every molecular species in STEMI HDL is shown as a colored bar relative to its mean abundance in control HDL. The color represents the direction and the magnitude of the between-group differences: red color corresponds to increases in the abundances of molecular species in patients vs controls, while violet color stays for their decreases. Lipid species are listed in the order of increasing backbone carbon chain length and double bond number within each lipid subclass (A, C) or in the order of increasing chain length independently of the lipid subclasses (B). Lipid abundances are expressed as wt% of total phospho- and sphingolipids measured. (For interpretation of the references to color in this figure legend, the reader is referred to the Web version of this article.)

differences were found throughout HDL subpopulations for Cer(d18:2/18:0), Cer(d18:2/16:0), Cer(d18:1/16:0), Cer(d18:1/18:0) and Cer (d18:1/14:0) species which were all significantly increased vs. controls, and PS 40:5 and 38:4 species which were significantly decreased (Fig. 1, C).

3.2. Minor species of PA, LPC, PC, SM and Cer were predominantly affected by STEMI in HDL subpopulations

Bubble plots are a type of charts similar to heatmaps, but containing additional information on the relative abundance of lipid species within a group. Extending upon the information provided by the heatmaps, the bubble plots revealed that abundances of numerous species of PA and LPC were consistently increased by up to 4.63 and 2.18-fold, respectively ($p < 0.001$) in STEMI HDLs as compared to their counterparts from controls (Fig. 2 and Fig. S1 from Data Supplement). By contrast, abundances of PC, SM and some Cer species were typically decreased by up to 3.14, 1.85 and 1.75-fold, respectively ($p < 0.001$) across HDL subpopulations. PE and PI species revealed mixed patterns involving both elevated and reduced abundances in STEMI vs. control HDL. Importantly, positive correlations between the magnitude of between-group difference for the species and their overall abundance in the HDL lipidome was observed for PC, SM and Cer lipids collectively ($r = 0.68, 0.61, 0.79, 0.66$ and 0.65 for HDL2b, 2a, 3a, 3b and 3c, respectively; $p < 0.005$ for all). On the contrary, LPC and PA species collectively avoided this trend, forming clusters in a seemingly random manner, or presenting with a counter-trend of negative correlations between the magnitude of difference between the groups and overall abundance in HDL lipidome, reaching significance in HDL2b ($r = -0.53$, $p < 0.05$), HDL3a ($r = -0.72$, $p < 0.05$) and HDL3b ($r = -0.49$, $p < 0.05$) subpopulations. Together with the heatmaps, the bubble plots thereby demonstrated that moderately and highly abundant, within their classes, PC, SM and Cer species were altered modestly, while low-abundant species of PC and PA, as well as moderately to highly-abundant species of LPC were altered more strongly in STEMI HDL.

3.3. Lipidomic alterations of HDL subpopulations in STEMI increased with increasing chain length and unsaturation level of affected species

The circular heatmap of phospholipids ordered in increasing number

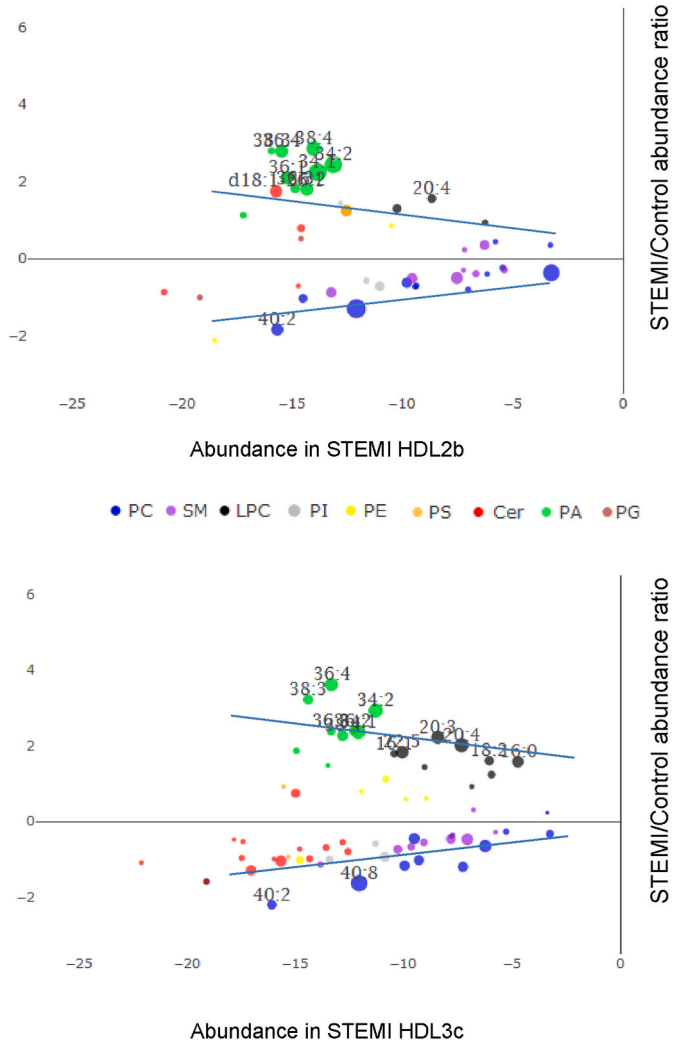

Fig. 2. Bubble plots of lipid species of large, light HDL2b and small, dense HDL3c subpopulations from STEMI patients in comparison to control subjects. Each colored bubble corresponds to a single species. Horizontal axis represents a log2 of the abundances of molecular species in the patient group; vertical axis represents log2 of the ratio of abundances of each molecular species in the patient and control groups. The y = 0 line separates the species that are increased in the patient group (above the line) from the species that are decreased (below the line) relative to controls. The size of each bubble is inversely proportional to the p value of the difference between the patient and control groups for the abundance of a given molecular species. Only species with p values of <0.05 for the between-group differences are included in the plots. Species with between-group abundance ratios of more than 2 or less than −2, and with between-group difference p values less than 0.01 are denoted by name tags showing their carbon backbone structure. Straight lines represent linear fitting through all the points shown above and below the y = 0 line. Lipid abundances are expressed as wt% of total phospho- and sphingolipids measured.

of double bonds reveals the structure of lipid species whose abundances significantly differed between the two groups. Cornucopia of unsaturated PC, LPC, PI, PE and PA species with multiple double bonds in their fatty acid moieties showed marked differences in their abundances between the patient and control groups, while differences in the HDL content of the species containing only SFA residues were less pronounced (Fig. 1). Indeed, among molecular species whose abundances significantly differed between the STEMI and control groups, 91% (31 of 34), 92% (46 of 50), 100% (23 of 23), 94% (50 of 53) and 93% (39 of 42) possessed at least one double bond in their fatty acid carbon chain residues in HDL2b, 2a, 3a, 3b and 3c, respectively. These data demonstrated that unsaturated molecular species were most strongly affected by STEMI, reflecting their predominance in the HDL lipidome (Tables S1 and S2 from Data Supplement).

Interestingly, intermediate- and long-chain species of PC, PI and PG were more strongly affected by STEMI than their short-chain counterparts (Fig. 2 and Fig. S2), resulting in positive correlations between their fold decrease in STEMI and the carbon chain length (e.g. r = 0.20, 0.27 and 0.23 for PC, PG and PI classes, respectively; all $p < 0.05$). In addition, the fold decrease in PE, PG and PI species was positively correlated with the number of double bonds (e.g. r = 0.40, 0.39 and 0.34 for PE, PG and PI, respectively; all $p < 0.01$).

While abundances of a majority of SM and Cer species affected in HDL supopulations by STEMI were decreased, those of the species containing 18:0, 19:0 and 26:1 fatty acid moieties were elevated relative to control HDLs (Fig. 3 and Tables S1 and S2 from Data Supplement). It is of note that very long-chain Cer and SM species were differentially affected by STEMI as compared to their long-chain counterparts as documented by the elevated ratio of the abundances of Cer(d18:1/18:0) and Cer(d18:1/24:0) species in STEMI HDLs (Fig. 4 and Table S3 from Data Supplement). This ratio tended to be positively correlated with plasma levels of hsCRP; this correlation reached significance in the HDL3a subpopulation (r = 0.62, $p < 0.05$).

3.4. *Biological activities of HDL subpopulations were associated with abundances of PL and Cer species*

Network maps offer a graph-type visual representation of all intrinsic correlations within a dataset. To elucidate the role of compositional alterations for biological properties of HDL, network analysis was performed for all correlations between functional metrics and individual lipid abundances in HDL particles.

Compositional relationships revealed a systematic pattern across HDL subpopulations. Interestingly, LPC and PA species, which were enriched in small, dense HDL3, clustered together, whereas PS, which was also enriched in HDL3, formed a separate cluster with some Cer species (Fig. 5, A). Two smaller clusters were built by PI and PG species, and most of the molecules belonging to other lipid classes, including PC, PE, SM and Cer, overlapped in a large cluster.

Cholesterol efflux capacity and antioxidative activity of HDLs were correlated with the abundances of only a few lipid species (Fig. 5B and C and D). Whereas antioxidative activity (measured as a decrease in the LDL oxidation rate in the propagation phase) was significantly and negatively associated with the abundances of PE 38:3 (p = 0.02), Cer d18:1/18:0 (p = 0.02) and Cer d18:1/19:0 (p = 0.03) species, cholesterol efflux capacity of HDLs was only positively associated with the abundance of PS 34:2 (p = 0.05). Remarkably, the two phospholipid species that revealed positive correlations with the two metrics of HDL functionality assessed in our study were both polyunsaturated.

Finally, the HDL lipidome was correlated with the metrics of glycemic control and inflammation (data not shown). Specifically, abundances of PC species largely revealed negative correlations with plasma glucose and hsCRP, while those of PA and PE species showed only positive correlations. Remarkably, abundances of PC 32:2 were negatively correlated with hsCRP across all five HDL subpopulations, while abundances of PC 36:2 and PC 40:8 were negatively correlated with glucose in four and three HDL subpopulations, respectively. Abundances of PE 38:3 and Cer d18:1/18:0 were positively associated with glucose and hsCRP in several HDL subpopulations, while those of SM 32:2 and SM 41:2 revealed negative associations.

3.5. *Pathways involving glycerophospholipid and linoleic acid metabolism in HDL subpopulations were affected by STEMI*

The list of lipid species whose abundances were correlated with the biological activities of HDL supopulations and were significantly different between the patient and control groups was entered into the

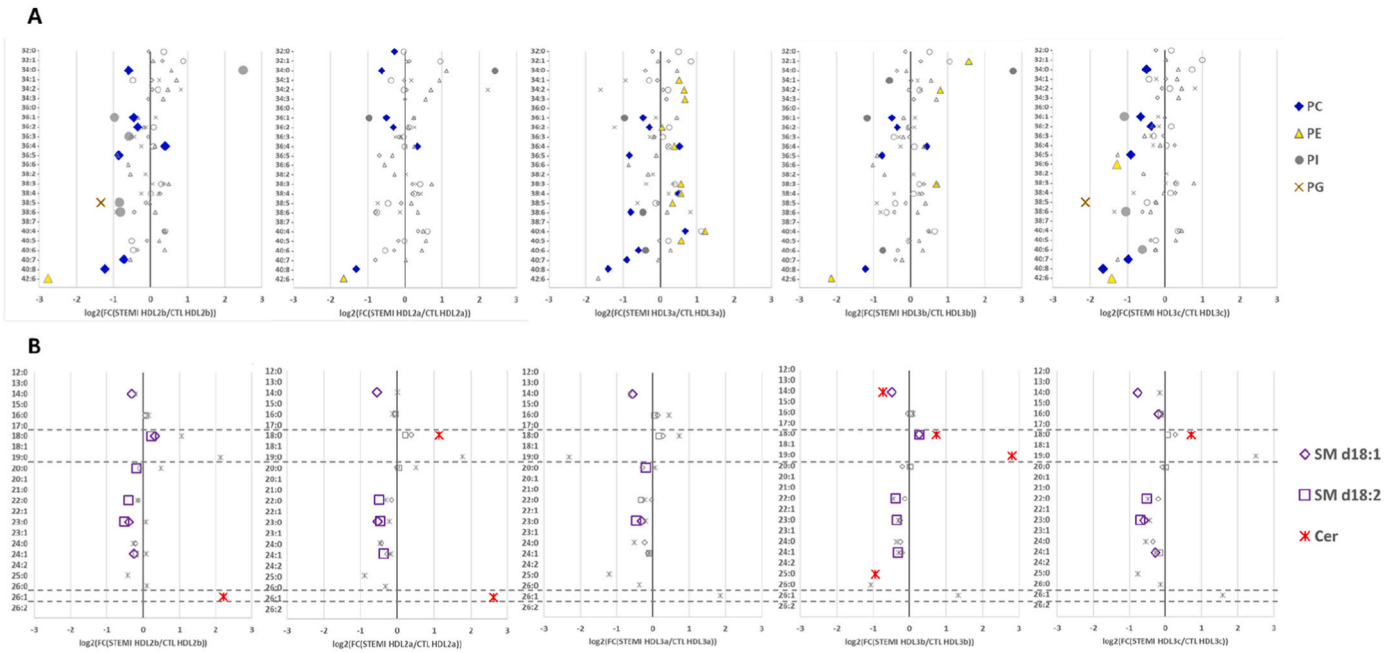

Fig. 3. Forest plots of differences in the abundance of phospholipid (A) and sphingolipid (B) species in the lipidome of HDL subpopulations of STEMI patients in comparison to healthy controls. Individual species of PC, PE, PI and PG are shown in panel A and individual species of SM d18:1, SM d18:2 and ceramides are in panel B. Lipid species are listed along the Y axis in the order of increasing backbone carbon chain length and double bond number. Lipid abundances are expressed as wt% of total phospho- and sphingolipids measured.

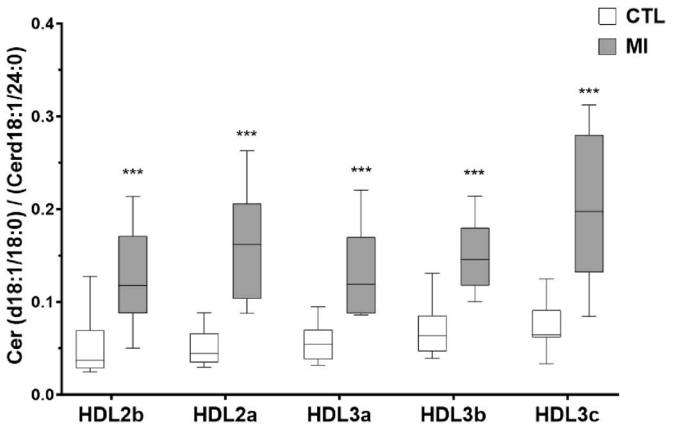

Fig. 4. Enrichment of HDL subpopulations in long-chain relative to very long-chain ceramide species in STEMI. Data are shown as the ratios (median and range) of the abundances of Cer(d18:1/18:0) and Cer(d18:1/24:0) species in HDL subpopulations from STEMI patients and healthy controls; ***$p < 0.001$ vs. corresponding control HDL subpopulation. CTL, control, MI, myocardial infarction.

MetExplore web server [24] in order to identify metabolic pathways altered by STEMI. The representation of the metabolic pathways identified was subsequently included in the classical pathway representation (Fig. 6 and Fig. S3 from Data Supplement). The list of affected pathways included inositol phosphate, glycerophospholipid, alpha-linolenic acid, glycosylphosphatidylinositol (GPI)-anchor and linoleic acid (LA) metabolism (Table S4 from Data Supplement), with 49 enzymes potentially involved (Table S5 from Data Supplement). Following the Benjamini-Hochberg correction, significant metabolic alterations were only detected for glycerophospholipid and LA metabolic pathways.

4. Discussion

In the present study, HDL particle subpopulations isolated from STEMI patients revealed markedly perturbed profile of individual phospholipid and sphingolipid species, adding to reduced plasma concentrations of HDL-C. Abundances of minor proinflammatory lysophospholipid species of LPC and PA were increased in STEMI HDLs, while abundances of minor species of PC, PG, PI, PE and SM were decreased. Importantly, the analysis of the abundances of lipid species uncovered distinct patterns in STEMI HDL subpopulations, which remained hidden in the analysis of the abundances of total phospho- and sphingolipid classes performed by us earlier [15]. Specifically, minor unsaturated intermediate-to-long-chain phospholipid and sphingolipid species were most affected by STEMI, reflecting alterations in glycerophospholipid and linoleic acid metabolism. These compositional alterations were specific for STEMI as indicated by the distinct remodelling of the lipidome of HDL subpopulations in patients with Metabolic Syndrome who presented with atherogenic dyslipidemia in the absence of acute phase response.

The perturbations of the phospho- and sphingolipidome of HDL subpopulations affected multiple species from all lipid classes. Among the species whose HDL content differed between the STEMI and control groups, the content of PC, SM and PI species was typically decreased, while that of LPC and PA species was rather increased in STEMI. PE, PS and Cer species revealed mixed patterns, with some species featuring elevated abundances, while other species characterized by reduced content in STEMI HDLs.

Interestingly, abundances of species from PC, SM and Cer classes were positively correlated with their between-group fold decrease throughout all HDL subpopulations. Futhermore, negative correlations between the abundances of LPC and PA lipids with their between-group increases were observed in HDL2b, HDL3a and HDL3b subpopulations. The first relationship indicates that the higher between-group differences for certain PC, SM or Cer species, the lower their abundance in the whole lipidome. The relationship observed for the LPC and PA species, though possessing the opposite sign, can be interpreted in a similar way as the positive trend found for the PC, SM and Cer species. This

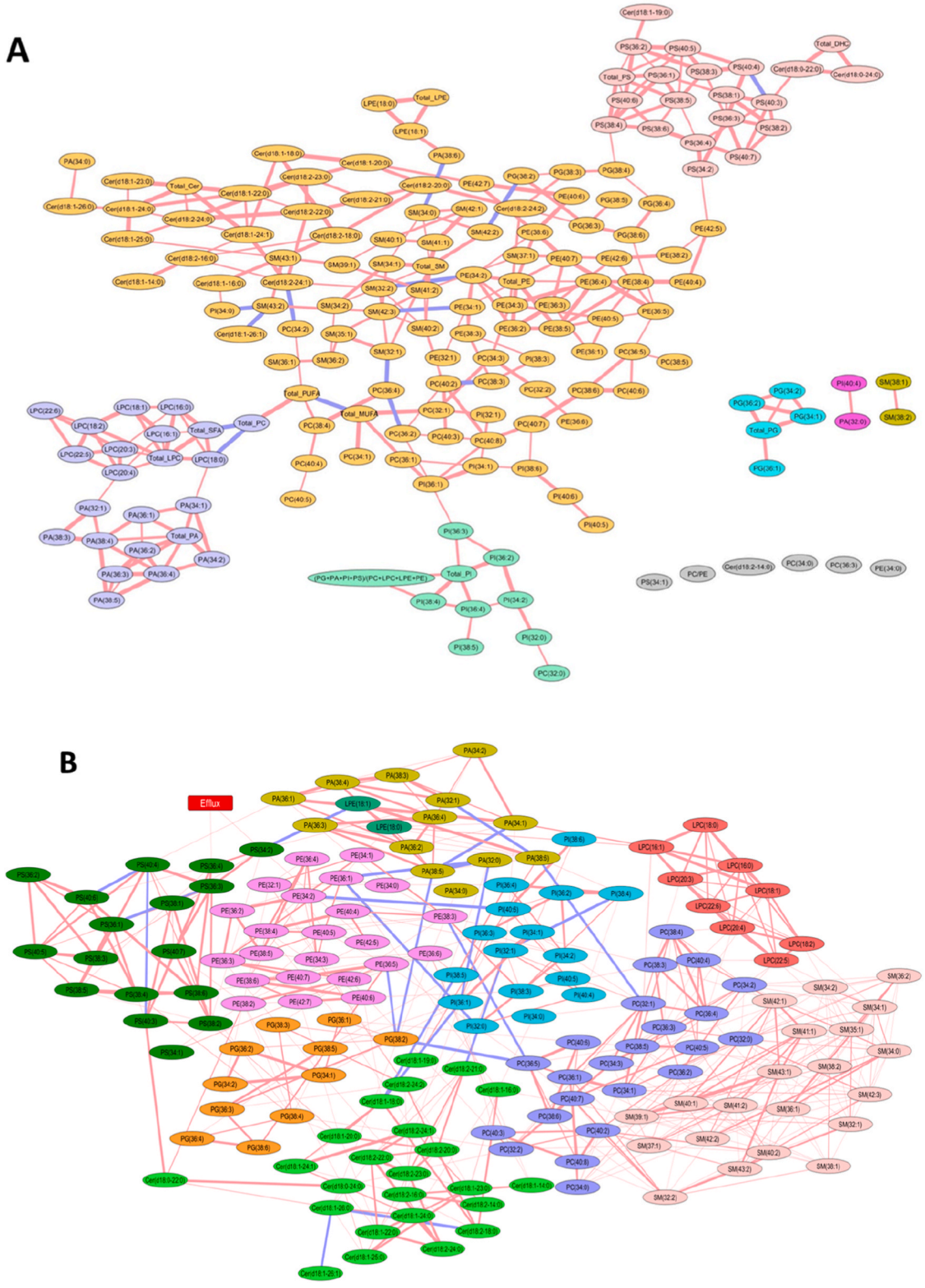

Fig. 5. Network maps of lipid species and biological activities of HDL subpopulations. Correlations between abundances of lipid species across five HDL subpopulations (A), between cholesterol efflux capacity and abundances of lipid species across five HDL subpopulations (B), between antioxidative activity and abundances of all lipid species in the HDL3b and 3c subpopulations (C), and between antioxidative activity of HDLs and the abundances of PE 38:3 ($r = -0.42$, $p = 0.02$), Cer d18:1/18:0 ($r = -0.31$, $p = 0.02$) and Cer d18:1/19:0 ($r = -0.44$, $p = 0.03$) as well as between cholesterol efflux capacity and the abundance of PS 34:2 ($r = 0.48$, $p = 0.05$) (D) are shown. Elliptic and rectangular nodes depict lipid species and biological activities, respectively. Distinct identified clusters (A) or different lipid classes (B and C) are represented in different colors. Thickness of a connection between two nodes is proportional to a correlation strength between them. Positive and negative correlations are shown as red and blue lines, respectively. Lipid abundances are expressed as wt% of total phospho- and sphingolipids measured. AOX RATE2, antioxdative activity of HDL calculated as % decrease in the propagation rate of LDL oxidation; Efflux, cholesterol efflux to HDL expressed as % of total radioactivity. (For interpretation of the references to color in this figure legend, the reader is referred to the Web version of this article.)

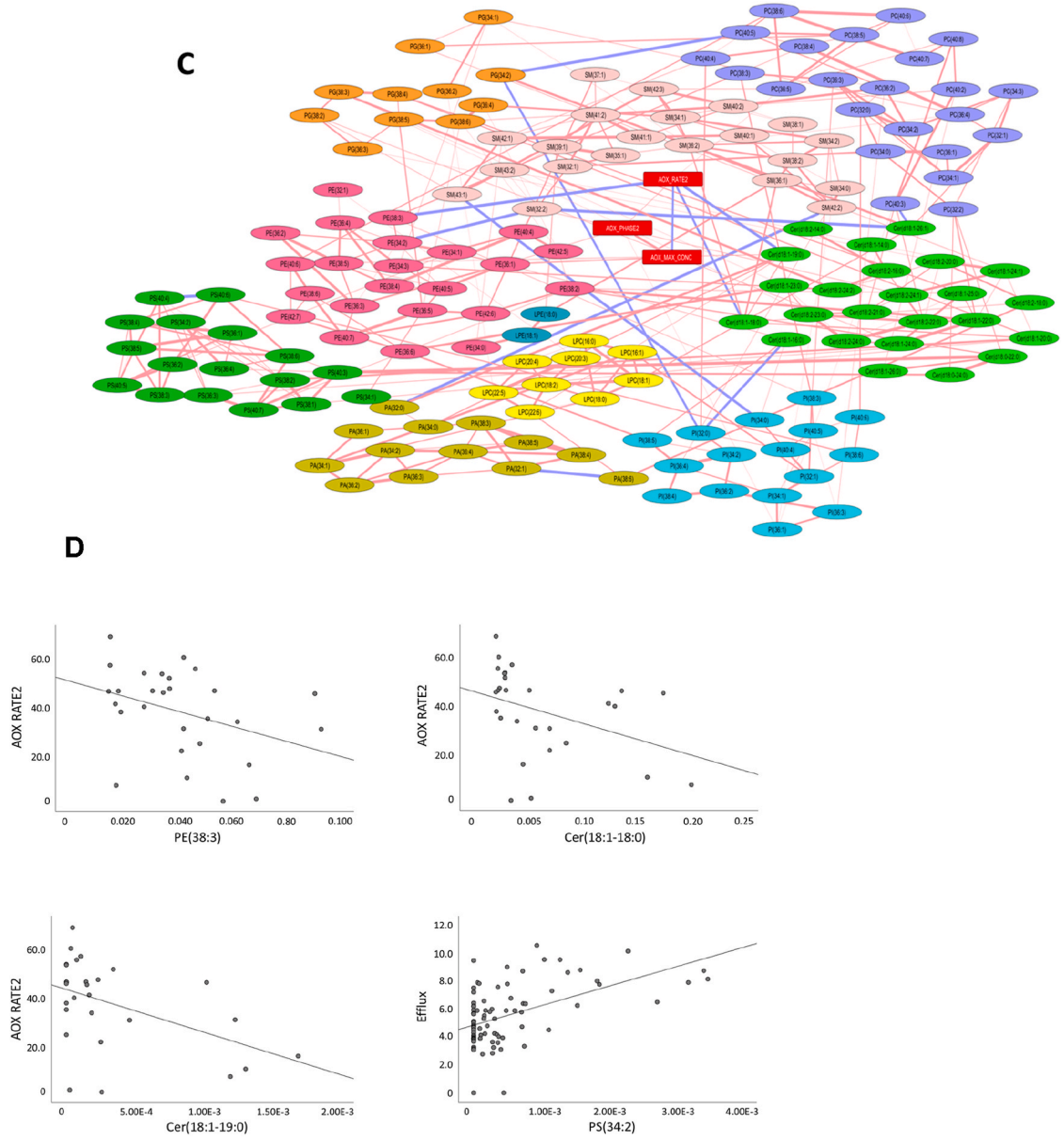

Fig. 5. (*continued*).

phenomenon can be termed a "backbone effect": major, in terms of overall abundance, species can be too vital for homeostasis to be significantly altered, while quantitatively minor species, though being far from minor in their biological role, are subject to volatility, with potentially deleterious effects on HDL function. Alternatively, their reduced content in HDL subpopulations may constitute a consequence rather than a cause of HDL functional deficiency.

In addition, we observed two other trends involving the relationships of HDL lipidomic alterations in STEMI with carbon chain length and double bond number of the affected species. The first trend was represented by intermediate- and long-chain species of PC, PI and PG displaying positive correlations between their fold decrease in STEMI and the carbon chain length. The second relationship included positive correlations between the fold decrease in the abundances of PE, PG and PI species with the number of double bonds. In conjunction with the backbone effect, its definition can thereby be expanded to specifically include alterations in minor long-chained species possessing at least one double bond in their fatty acid moieties.

Remarkably, STEMI HDL subpopulations lacked numerous relatively abundant polyunsaturated lipid species of PC, including PC 36:2 and PC 38:5, while possessing increased amounts of less abundant saturated species of LPC and PA, including LPC 16:0, LPC 18:0 and PA 32:0. These compositional alterations were most pronounced in small, dense HDL3 particles which display potent biological activities [14]. Importantly, cluster analysis revealed that multiple species of LPC and PA clustered together, suggesting their common association with pro-inflammatory activation of lipolytic pathwyas in STEMI [15]. Indeed, it is generally accepted that SFAs exert proinflammatory actions [25]; moreover, LPC is well-known to possess proinflammatory properties [26] and to display a high affinity for G-protein-coupled receptors, thereby playing a signaling role [27–29], while PA participates in the regulation of inflammation [30] and intracellular signaling [31]. We [15] and others [18] already reported increased LPC content in HDL of ACS patients. Ischemia and increased oxidative stress are key features of acute myocardial infarction [32]. It is therefore reasonable to assume that enhanced oxidation of PUFAs is at least partially responsible for their decreased content in STEMI HDL [33]. Indeed, oxidative stress may play a role in the impairment of HDL function [32]. Although a whole array

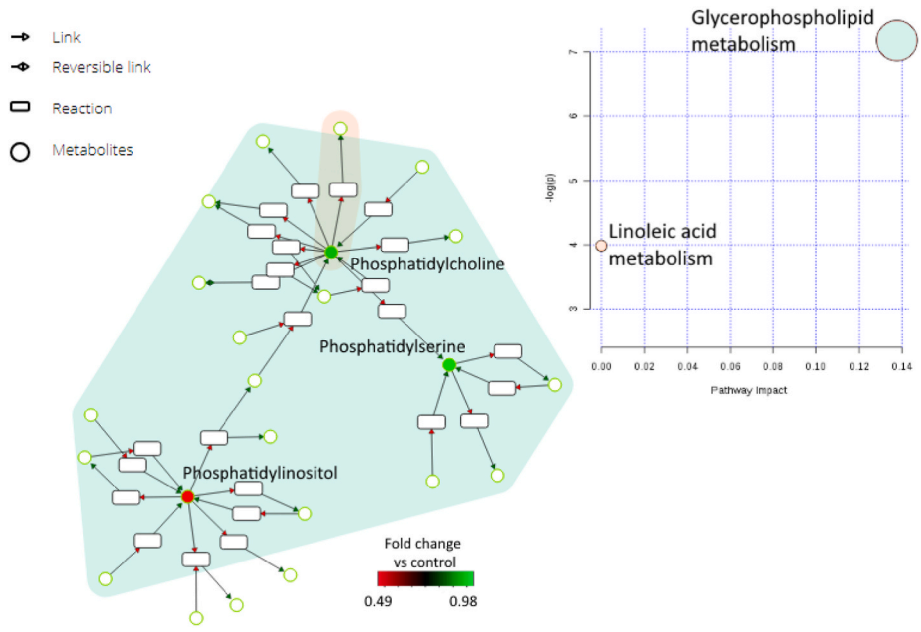

Fig. 6. Metabolic pathways associated with alterations of the HDL lipidome in STEMI, extracted using MetExplore. Inset denotes the impact of identified pathways (X axis) in relationship to its significance (Y axis) produced using MetaboAnalyst. Colors in the graph highlight affected pathways and correspond to the colors of the circles in the inset. Green and red circles in the graph denote increased and decreased abundances vs. controls, respectively, with color scale shown at the bottom of the graph. (For interpretation of the references to color in this figure legend, the reader is referred to the Web version of this article.)

of LPC and PA species was enriched in STEMI HDL particles, the structure-function analysis did not reveal their direct links with HDL function evaluated as cholesterol efflux capacity and antioxidative activity. The species of the proatherogenic duo of LPC and PA may therefore have acted indirectly by promoting formation of a pro-inflammatory milieu and further deteriorating HDL functionality already hampered by altered particle composition. The imbalance of PUFA relative to SFA species found in the present study may have contributed to already elevated systemic inflammation naturally occurring in STEMI as observed by us.

Interestingly, alterations of HDL sphingolipids revealed a complex pattern in STEMI. Indeed, while most sphingolipid species were depleted in STEMI HDLs, sphingolipids containing 18:0 and 26:1 fatty acid moieties were enriched. These species-specific effects might reflect differential activities of specific ceramide synthase isoforms as suggested by the alterations in the Cer(d18:1/18:0)/Cer(d18:1/24:0) ratio. Ceramides containing fatty acid moieties of 16 and 18 carbon atoms exert deleterious cardiometabolic effects [29] and their circulating levels are associated with cardiovascular death [30]. By contrast, very long chain ceramides containing fatty acid moieties which are 24 and 26 carbon atom long are rather associated with beneficial outcomes. The Cer (d18:1/18:0)/Cer(d18:1/24:0) ratio might therefore represent a biomarker of altered sphingolipid metabolism in STEMI.

Using a network analysis we attempted to elucidate structure-function relationships across HDL particle subpopulations in STEMI patients and normolipidemic controls. When plotted as a part of a correlation network map, LPC and PA species formed a distinct cluster, while three separate clusters primarily involving PS, Cer, PI and PG species were observed. This clustering pattern might be attributed to similar differences in the phosphosphingolipidome between different HDL subpopulations as found for lipid species of LPC, PA and PS which were all enriched in small, dense HDL3. It is interesting to mention in this regard that the lipidome of small, dense HDL3 particles was more strongly affected by STEMI as compared to that of large, light HDL2.

Combined with functional characteristics of HDL, the network analysis demonstrated that antioxidative activity was linked to the abundances of one PE and two Cer species, while cholesterol efflux capacity was only associated with a single PS molecule. These data suggest that PE, Cer and PS species additionally contributed to functional deficiency of HDL particle subpopulations in STEMI. Interestingly, the both phospholipid species whose HDL content was linked to functional properties of HDLs carried two or more double bonds in their fatty acid moieties, consistent with a potential pathophysiological role of polyunsaturated lipids discussed above.

We further employed *ab intitio* metabolic pathway analysis to identify pathways affected in the metabolism of STEMI HDL particles. Our approach revealed that glycerophospholipid and LA metabolic pathways were both altered in STEMI. Glycerophospholipid metabolism is reportedly associated with atherosclerosis progression, with distinct plasma metabolomic profiles differentiating between different stages of atherosclerosis [34]. Glycerophospholipids represent a common class of lipids critically important for the integrity of cellular membranes; oxidation of esterified PUFA moieties dramatically alters biological activities of phospholipids [35]. As observed by us, STEMI HDL particles displayed reduced antioxidative activity [15], potentially reflecting their increased content of pro-inflammatory lipids LPC and PA.

LA metabolism is tightly linked to atherogenesis through multiple anti-atherogenic activities of LA. Indeed, conjugated LAs can reduce concentrations of atherogenic lipoproteins in the circulation and attenuate inflammation [36]. In addition, LA displays protective effects against cholesterol accumulation in human macrophages [37]. Dietary supplementation of LA-rich fat, compared with a SFA-rich fat in apoE-deficient mice, led to lowered atherosclerosis, reduced serum total cholesterol levels, increased HDL-C and attenuated hepatic cholesterol content [38].

We feel the necessity to acknowledge that our study is not free of limitations, as the causality of the alterations in the HDL lipidome for the HDL function was not elucidated in the present work. It is not clear whether the dysfunction of STEMI HDL particles causes its lipidome to accumulate lipids that further promote degeneration of its anti-atherogenic properties, or whether such compositional alterations occur before cardiac events that provoke the eventual functional deficiency of HDL particles which we observed in STEMI. Another limitation was that our analysis did not allow distinguishing between individual molecular

species of phospholipids but rather between isobaric structural isomers instead. Finally, the study was exclusively performed in male subjects, which limits applicability of our findings to males.

In conclusion, our findings presented herein document multiple alterations in the lipidomic composition and their links to functionality of HDL particle subpopulations in STEMI. Multiplied by low circulating HDL concentrations, such deficiency in HDL composition and function can be expected to contribute to accelerated atherogenesis observed in this clinical condition. Indeed, similar abnormalities of the HDL lipidome occur under conditions associated with elevated cardiovascular risk, including familial apoA-I deficiency [39] and insulin resistance [22, 23]. As a corollary, normalization of HDL phospho- and/or sphingolipid composition (i.e. via HDL enrichment in functional phospho- and/or sphingolipids through a diet or medical intervention), may represent a therapeutic strategy to further reduce cardiovascular risk in STEMI. Our findings may therefore be of a clinical relevance as they bear a potential to normalize lipoprotein metabolism and diminish cardiovascular risk in STEMI.

Financial Support

These studies were supported by CAPES (Brazil), FAPESP (Brazil), National Institute of Health and Medical Research (INSERM, France) and Russian Science Foundation (Grant # 18-15-00254). F.R. acknowledges financial support from the “Association pour la Recherché sur les Lipoproteines et l’Atherogenese” (ARLA, France). M.L. acknowledges the support of the Fondation pour la Recherche Médicale (Paris, France). M.J.C. and A.K. received research grant funding from CSL (Australia). R.D.S. received honoraria consulting or speakers engagements from the following companies: Astra Zeneca, Amgen, Aegerion, Biolab, Boehringer Ingelheim, Bristol-Myers Squibb, Genzyme, Unilever, Pfizer, Lilly, Novo Nordisk, Novartis and Sanofi.

Author contributions

Designing research studies: FR, CVS, RDS, MJC, AO, AK. Providing financial support: CVS, RDS, MJC, AO, AK. Recruiting study subjects: FR, CVS, RDS. Conducting measurements: ML, LC, FR. Acquiring data: ML, FR. Analysing data: MP, EZ, ML, AK. Writing the manuscript: EZ, ML, MJC, AK.

Declaration of competing interest

The authors declare that they have no known competing financial interests or personal relationships that could have appeared to influence the work reported in this paper.

Appendix A. Supplementary data

Supplementary data to this article can be found online at https://doi.org/10.1016/j.athplu.2023.12.001.

References

[1] Boren J, Williams KJ. The central role of arterial retention of cholesterol-rich apolipoprotein-B-containing lipoproteins in the pathogenesis of atherosclerosis: a triumph of simplicity. Curr Opin Lipidol 2016;27:473–83.
[2] Roe MT, Ou FS, Alexander KP, Newby LK, Foody JM, Gibler WB, Boden WE, Ohman EM, Smith Jr SC, Peterson ED. Patterns and prognostic implications of low high-density lipoprotein levels in patients with non-ST-segment elevation acute coronary syndromes. Eur Heart J 2008;29:2480–8.
[3] Perez-Mendez O, Pacheco HG, Martinez-Sanchez C, Franco M. HDL-cholesterol in coronary artery disease risk: function or structure? Clin Chim Acta 2014;429:111–22.
[4] Soares AAS, Tavoni TM, de Faria EC, Remalay AT, Maranhao RC, Sposito AC. HDL acceptor capacities for cholesterol efflux from macrophages and lipid transfer are both acutely reduced after myocardial infarction. Clin Chim Acta 2018;478:51–6.
[5] Brites F, Martin M, Guillas I, Kontush A. Antioxidative activity of high-density lipoprotein (HDL): mechanistic insights into potential clinical benefit. BBA Clin 2017;8:66–77.
[6] Riwanto M, Rohrer L, Roschitzki B, Besler C, Mocharla P, Mueller M, Perisa D, Heinrich K, Altwegg L, von Eckardstein A, Luscher TF, Landmesser U. Altered activation of endothelial anti- and proapoptotic pathways by high-density lipoprotein from patients with coronary artery disease: role of high-density lipoprotein-proteome remodeling. Circulation 2013;127:891–904.
[7] Sorrentino SA, Besler C, Rohrer L, Meyer M, Heinrich K, Bahlmann FH, Mueller M, Horvath T, Doerries C, Heinemann M, Flemmer S, Markowski A, Manes C, Bahr MJ, Haller H, von Eckardstein A, Drexler H, Landmesser U. Endothelial-vasoprotective effects of high-density lipoprotein are impaired in patients with type 2 diabetes mellitus but are improved after extended-release niacin therapy. Circulation 2010;121:110–22.
[8] Gomaraschi M, Ossoli A, Favari E, Adorni MP, Sinagra G, Cattin L, Veglia F, Bernini F, Franceschini G, Calabresi L. Inflammation impairs eNOS activation by HDL in patients with acute coronary syndrome. Cardiovasc Res 2013;100:36–43.
[9] Khera AV, Demler OV, Adelman SJ, Collins HL, Glynn RJ, Ridker PM, Rader DJ, Mora S. Cholesterol efflux capacity, high-density lipoprotein particle number, and incident cardiovascular events: an analysis from the JUPITER trial (justification for the use of statins in prevention: an intervention trial evaluating rosuvastatin). Circulation 2017;135:2494–504.
[10] Kavo AE, Rallidis LS, Sakellaropoulos GC, Lehr S, Hartwig S, Eckel J, Bozatzi PI, Anastasiou-Nana M, Tsikrika P, Kypreos KE. Qualitative characteristics of HDL in young patients of an acute myocardial infarction. Atherosclerosis 2012;220:257–64.
[11] Dullaart RP, Annema W, Tio RA, Tietge UJ. The HDL anti-inflammatory function is impaired in myocardial infarction and may predict new cardiac events independent of HDL cholesterol. Clin Chim Acta 2014;433:34–8.
[12] Alwaili K, Bailey D, Awan Z, Bailey SD, Ruel I, Hafiane A, Krimbou L, Laboissiere S, Genest J. The HDL proteome in acute coronary syndromes shifts to an inflammatory profile. Biochim Biophys Acta 2012;1821:405–15.
[13] Vaisar T, Tang C, Babenko I, Hutchins P, Wimberger J, Suffredini AF, Heinecke JW. Inflammatory remodeling of the HDL proteome impairs cholesterol efflux capacity. J Lipid Res 2015;56:1519–30.
[14] Camont L, Chapman MJ, Kontush A. Biological activities of HDL subpopulations and their relevance to cardiovascular disease. Trends Mol Med 2011;17:594–603.
[15] Rached F, Lhomme M, Camont L, Gomes F, Dauteuille C, Robillard P, Santos RD, Lesnik P, Serrano Jr CV, Chapman MJ, Kontush A. Defective functionality of small, dense HDL3 subpopulations in ST segment elevation myocardial infarction: relevance of enrichment in lysophosphatidylcholine, phosphatidic acid and serum amyloid A. Biochim Biophys Acta 2015;1851:1254–61.
[16] Kostara CE, Papathanasiou A, Psychogios N, Cung MT, Elisaf MS, Goudevenos J, Bairaktari ET. NMR-based lipidomic analysis of blood lipoproteins differentiates the progression of coronary heart disease. J Proteome Res 2014;13:2585–98.
[17] Sutter I, Velagapudi S, Othman A, Riwanto M, Manz J, Rohrer L, Rentsch K, Hornemann T, Landmesser U, von Eckardstein A. Plasmalogens of high-density lipoproteins (HDL) are associated with coronary artery disease and anti-apoptotic activity of HDL. Atherosclerosis 2015;241:539–46.
[18] Lee JH, Yang JS, Lee SH, Moon MH. Analysis of lipoprotein-specific lipids in patients with acute coronary syndrome by asymmetrical flow field-flow fractionation and nanoflow liquid chromatography-tandem mass spectrometry. J Chromatogr, B: Anal Technol Biomed Life Sci 2018;1099:56–63.
[19] Meikle PJ, Formosa MF, Mellett NA, Jayawardana KS, Giles C, Bertovic DA, Jennings GL, Childs W, Reddy M, Carey AL, Baradi A, Nanayakkara S, Wilson AM, Duffy SJ, Kingwell BA. HDL phospholipids, but not cholesterol distinguish acute coronary syndrome from stable coronary artery disease. J Am Heart Assoc 2019;8:e011792.
[20] Ding M, Rexrode KM. A review of lipidomics of cardiovascular disease highlights the importance of isolating lipoproteins. Metabolites 2020;10.
[21] Kostara CE, Bairaktari ET, Tsimihodimos V. Effect of clinical and laboratory parameters on HDL particle composition. Int J Mol Sci 2023;24.
[22] Stahlman M, Fagerberg B, Adiels M, Ekroos K, Chapman JM, Kontush A, Boren J. Dyslipidemia, but not hyperglycemia and insulin resistance, is associated with marked alterations in the HDL lipidome in type 2 diabetic subjects in the DIWA cohort: impact on small HDL particles. Biochim Biophys Acta 2013;1831:1609–17.
[23] Denimal D, Monier S, Bouillet B, Vergès B, Duvillard L. High-density lipoprotein alterations in type 2 diabetes and obesity. Metabolites 2023;13.
[24] Jourdan F, Cottret L, Huc L, Wildridge D, Scheltema R, Hillenweck A, Barrett MP, Zalko D, Watson DG, Debrauwer L. Use of reconstituted metabolic networks to assist in metabolomic data visualization and mining. Metabolomics 2010;6:312–21.
[25] Quehenberger O, Dennis EA. The human plasma lipidome. N Engl J Med 2011;365:1812–23.
[26] Marathe GK, Pandit C, Lakshmikanth CL, Chaithra VH, Jacob SP, D'Souza CJ. To hydrolyze or not to hydrolyze: the dilemma of platelet-activating factor acetylhydrolase. J Lipid Res 2014;55:1847–54.
[27] Xu H, Valenzuela N, Fai S, Figeys D, Bennett SA. Targeted lipidomics - advances in profiling lysophosphocholine and platelet-activating factor second messengers. FEBS J 2013;280:5652–67.
[28] Zmijewski JW, Landar A, Watanabe N, Dickinson DA, Noguchi N, Darley-Usmar VM. Cell signalling by oxidized lipids and the role of reactive oxygen species in the endothelium. Biochem Soc Trans 2005;33:1385–9.
[29] Litvack ML, Palaniyar N. Review: soluble innate immune pattern-recognition proteins for clearing dying cells and cellular components: implications on exacerbating or resolving inflammation. Innate Immun 2010;16:191–200.

[30] Lim HK, Choi YA, Park W, Lee T, Ryu SH, Kim SY, Kim JR, Kim JH, Baek SH. Phosphatidic acid regulates systemic inflammatory responses by modulating the Akt-mammalian target of rapamycin-p70 S6 kinase 1 pathway. J Biol Chem 2003; 278:45117–27.
[31] Delon C, Manifava M, Wood E, Thompson D, Krugmann S, Pyne S, Ktistakis NT. Sphingosine kinase 1 is an intracellular effector of phosphatidic acid. J Biol Chem 2004;279:44763–74.
[32] Bounafaa A, Berrougui H, Ikhlef S, Essamadi A, Nasser B, Bennis A, Yamoul N, Ghalim N, Khalil A. Alteration of HDL functionality and PON1 activities in acute coronary syndrome patients. Clin Biochem 2014;47:318–25.
[33] Garcia C, Montée N, Faccini J, Series J, Meilhac O, Cantero AV, Le Faouder P, Elbaz M, Payrastre B, Vindis C. Acute coronary syndrome remodels the antiplatelet aggregation properties of HDL particle subclasses. J Thromb Haemostasis 2018;16: 933–45.
[34] Dang VT, Huang A, Zhong LH, Shi Y, Werstuck GH. Comprehensive plasma metabolomic analyses of atherosclerotic progression reveal alterations in glycerophospholipid and sphingolipid metabolism in apolipoprotein E-deficient mice. Sci Rep 2016;6:35037.
[35] Bochkov VN, Oskolkova OV, Birukov KG, Levonen AL, Binder CJ, Stockl J. Generation and biological activities of oxidized phospholipids. Antioxidants Redox Signal 2010;12:1009–59.
[36] Stachowska E, Siennicka A, Baskiewcz-Halasa M, Bober J, Machalinski B, Chlubek D. Conjugated linoleic acid isomers may diminish human macrophages adhesion to endothelial surface. Int J Food Sci Nutr 2012;63:30–5.
[37] Song Y, Zhang LJ, Li H, Gu Y, Li FF, Jiang LN, Liu F, Ye J, Li Q. Polyunsaturated fatty acid relatively decreases cholesterol content in THP-1 macrophage-derived foam cell: partly correlates with expression profile of CIDE and PAT members. Lipids Health Dis 2013;12:111.
[38] Sato M, Shibata K, Nomura R, Kawamoto D, Nagamine R, Imaizumi K. Linoleic acid-rich fats reduce atherosclerosis development beyond its oxidative and inflammatory stress-increasing effect in apolipoprotein E-deficient mice in comparison with saturated fatty acid-rich fats. Br J Nutr 2005;94:896–901.
[39] Zakiev E, Rached F, Lhomme M, Darabi-Amin M, Ponnaiah M, Becker PH, Therond P, Serrano Jr CV, Santos RD, Chapman MJ, Orekhov A, Kontush A. Distinct phospholipid and sphingolipid species are linked to altered HDL function in apolipoprotein A-I deficiency. J Clin Lipidol 2019;13:468–480.e468.